Preamble-Less Carrier Phase Recovery in Rayleigh and Rician Channels

Mohamed K. Nezami
J. Bard
R. Sudhakar[1]
Mnemonics, Inc.
Melbourne, Florida

ABSTRACT

This paper reports the modeling, analysis, and simulation results of a preamble-less open loop carrier phase synchronization algorithm operating in a Rician fading environment on satellite channels subject to additive white Gaussian noise (AWGN). Furthermore, degradation effects due to frequency offset residual on the phase recovery algorithm is analyzed.

INTRODUCTION

One of the attractive features of a feed-forward (FF) synchronization algorithm is the absence of hang up and cycle slips, problems that feedback synchronizers suffer from. Another advantage is that the FF synchronizer can be fully implemented using DSP techniques and tested in separate modules, as there is no feedback from the synchronizer to the receiver front end.

The synchronization process in wireless receivers is implemented in the following order: estimate timing offset first [3,4], followed by frequency offset [5], and finally phase rotational offsets. In other words, frequency-offset estimation (and correction) assumes a signal with negligible timing errors, while phase estimation (and correction) assumes negligible frequency variation during the estimation interval. However, practical transmission systems have frequency-offset errors due to Doppler or the imperfect performance of the prior frequency-offset estimator. This results in degradation of the phase estimates, which then effects the receiver bit error rate. An optimal observation length can be found, which minimizes the effect of such residuals on carrier phase estimation.

One important performance measure of the such algorithm is its ability to operate reliably under Rayleigh and Rician fading or signal shadowing environments. Such channel distortion is caused either by the propagation effects associated with mobile, aircraft, or ship movement with respect to the satellite. For an aircraft moving at a velocity of 1000 km/hr, its satellite receiver reception is dominated by diffused signals resulting from reflections off the Earth's surface below. These reflections have large spread delays when compared to the direct path, resulting in a very large ISI distortion. Such situation is considered Rician channel with a Rician factor of 10-15 dB and a fading bandwidth of 30-100 Hz. Due to the Earth's surface roughness, this channel also is a frequency selective channel. Furthermore, Doppler frequency shifts are also present. These can be as high as 2 kHz at L-band. The Doppler is worse for low orbit satellites (LEO), where the shift can be as high as 10 kHz.

OPEN LOOP CARRIER PHASE ESTIMATOR

The use of a preamble reduces transmission efficiency for short-burst transmission systems, such as a PCS mobile system. Moreover, the performance of the carrier synchronizer depends on the receiver's capability in correctly detecting the preamble inserted within the transmitted burst. This limits the synchronizer's performance at low SNRs. An alternative to preamble-based synchronizers is the use of feed-forward preamble-less synchronization algorithms, which does not require any deterministic pattern, and works well for low SNRs.

Figure 1 shows one proposed carrier phase recovery scheme, it is assumed that frequency offsets have been estimated and corrected by a previous processing stage [5].

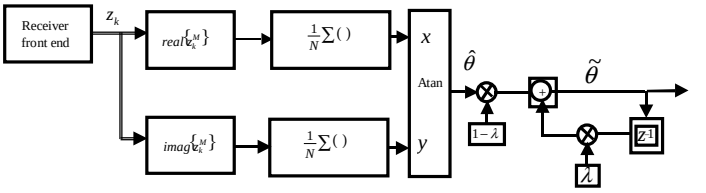

Figure 1. Phase Recovery Algorithm

The algorithm does not utilize a preamble and does not use feedback recovery methods, which causes instability and slow convergence rate. Instead it processes the random received symbols through an M power non-linearity, which removes phase modulations due to symbols, but leaves a signal from which phase information can be extracted. Carrier phase correction is achieved by the use of complex phase multipliers, in

[1] Dr. Sudhakar is full-time faculty at Florida Atlantic University.

conjunction with a direct digital synthesizer [5]. The phase algorithm implemented in the figure first computes phase offset $\hat{\theta}$ for an *N* observed received symbol samples using equation 2.

$$\hat{\theta} = \frac{1}{M}\tan^{-1}\left\{\frac{\sum_{k=0}^{N-1} imag\{z_k^M\}}{\sum_{k=0}^{N-1} real\{z_k^M\}}\right\} \quad (1)$$

where z_k is the matched filter output signal samples and *M* is chosen based on the type of modulations used. For QPSK *M=4*, and for BPSK *M=2*. The estimates are then smoothed using a linear least square filter, which is also a first-order Kalman filter [3]. Such a filter introduces feedback, yet it is important to reduce the effect of signal shadowing on phase estimates. Its bandwidth (time constant) can be chosen based on variance minimization iterative trial and error or based on the average signal-shadowing rate. The estimate post processing is defined as:

$$\tilde{\theta}(k) = \lambda\hat{\theta}(k) + (1-\lambda)\hat{\theta}(k-1) \quad (2)$$

where, $0 \le \lambda \ge 1$ is used to control the convergence rate. Figure 2 shows the frequency estimates for a QPSK satellite system running 10 kbps with an oversampling rate of 4 and an observation length of 50 symbols for an intentionally-introduced 10-degree phase error.

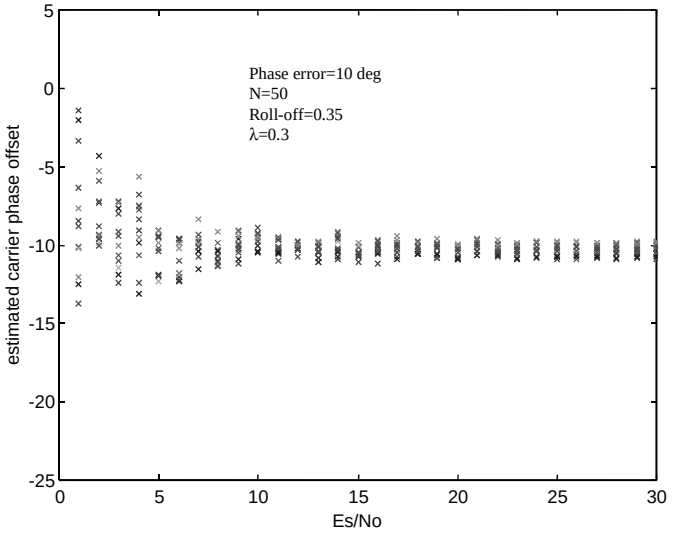

Figure 2. Estimation of 10° Error

To assess and be able to determine the optimal parameters for the proposed algorithm in terms of observation interval and smoothing filter timing constant, one must analyze phase error density for various channels such as AWGN, fading, shadowing, and the presence of a frequency residual error. Such analysis will yield statistical measures of the error distribution which then enables design engineers to better specify and design optimal phase carrier recovery algorithms, further giving minimal degradation while operating under shadowing and fading.

Estimated Phase Error Density in AWGN Channels

One way to evaluate the performance of the proposed algorithm is through the variance of the error estimates. Such parameters can be used to determine bit error deterioration [4] contributed by the imperfect operation of carrier phase estimator. Experimentally this can be obtained through simulations, where the random burst data is used in conjunction with an intentionally introduced phase error used (Figure 1) to estimate the phase error. By accumulating a number of such estimates, the variance can then be calculated. This variance is bounded by a lower bound known as the Modified Cramer-Rao Bound [4]. Analytically, the variance can also be found from the phase error density function. The density function is obtained by evaluating the joint probability of estimated phase and the amplitude distribution of the receiver signal. Depending on the channel, the amplitude distribution can vary, for AWGN it's Gaussian, while for faded signal, it's either Rayleigh or Rician distribution. Observing N-samples of the received signal defined as:

$$r(t) = s(t) + n(t) \quad (3)$$

where, $s(t)$ is the useful information signal and $n(t)$ is a complex white Gaussian noise with a zero mean and variance σ_n^2. For phase modulated signals such as QPSK and BPSK, the transmitted information signal can be represented by $s(t) = a(t)e^{j(2\pi f_c t + \theta(t))}$; where $a(t)$ is the information to be transmitted, f_c is the operating carrier frequency and $\theta(t)$ is the phase due to carrier rotation that has to be estimated. Unlike fading channels, for AWGN channels it is assumed that the signal's envelope and carrier phase are constant within the observation interval, or $a(t) = a$, and $\theta(t) = \theta$.

The quadrature signal at the averaged non-linearity output in Figure 3 is given by:

$$x = \frac{1}{N}\sum_{k=0}^{N-1} real(z_k^M)\ ,\ y = \frac{1}{N}\sum_{k=0}^{N-1} imag(z_k^M) \quad (4)$$

In the following analysis, without loss of generality, it can be assumed that $\theta = 0^0$ and therefore the error in carrier phase estimation is $\varphi = \hat{\theta}$. The envelope of the signal into the phase estimation algorithm is given by $R = \sqrt{x^2 + y^2}$

and estimation error given by φ, the joint density function of the amplitude phase error is given by:

$$P(R,\varphi)=\frac{e^{-\gamma/2}R}{2\pi\sigma_n^2}\exp\left[-\frac{R^2}{2\sigma_n^2}+\frac{\sqrt{\gamma}R\cos\varphi}{\sigma_n}\right] \quad (5)$$

where, the signal-to-noise ratio is defined:

$$\gamma=\frac{a^2/2}{\sigma_n^2} \quad (6)$$

Equation (5) can be used to derive the phase error density function that then can lead to analytical evaluation of the phase error variance.

$$P(\varphi)=\frac{e^{-\gamma/2}}{2\pi\sigma_n^2}\int_0^{\infty}R.\exp\left[-\frac{R^2}{2\sigma_n^2}+\frac{\sqrt{\gamma}R\cos\varphi}{\sigma_n}\right]dR \quad (7)$$

Equation (7) is further evaluated to yield:

$$p(\varphi)_N=\frac{e^{-N\gamma}}{2\pi}\{\,1+\sqrt{4\pi N\gamma}\cos\varphi \exp(\gamma N\cos^2\varphi)Q\left(-\sqrt{2\pi N\gamma}\cos\varphi\right)\,\} \quad (8)$$

The subscript *N* indicates that the calculation is performed using N numbers of observed symbols. Figure 3 shows this phase density function evaluated for an AWGN channel using several values of γ of 0, 3, 6, 9 and 15 dB for N=1.

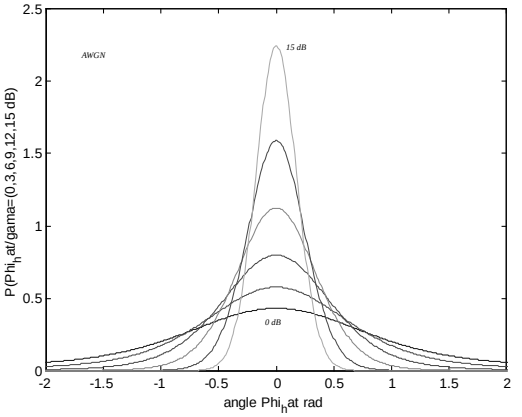

Figure 3. Phase Error Density

Notice how the error distribution changes linearly with SNR variation. Using γ = 15 dB, Figure 4 shows the effect of using a larger number of symbols, where N is 1, 10, 100, and 1000 symbols.

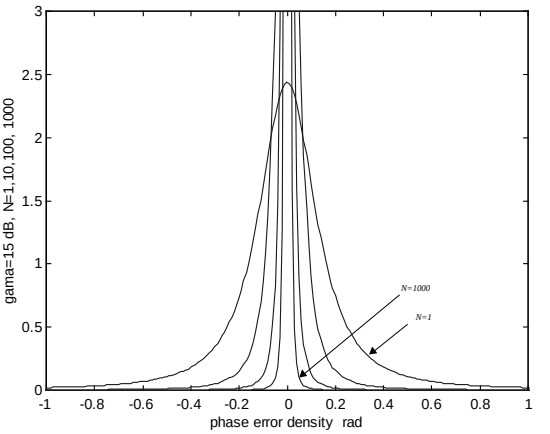

Figure 4. Phase Error Density

Clearly, phase error density function improves (gets narrower) as N increases. Phase error variance at the output of the estimator in Figure 1 can be estimated by numerically integrating (9).

$$\langle\varphi^2\rangle=\int_{-\pi}^{\pi}\varphi^2 p(\varphi)d\varphi \quad (9)$$

Finally, evaluating equation 9 for an AWGN channel leads to the Cramer-Rao lower bound [3] given by:

$$\langle\varphi^2\rangle=\frac{1}{2\gamma N} \quad (10)$$

Estimated Phase Error Density in Fading Channels

For Rayleigh and Rician channels, we can no longer consider the phase or the amplitude of the signal into the synchronizer to be constant, therefore equation (10) can no longer serve as a lower bound on the estimates nor be used to predict BER deterioration. Instead, the amplitude will have either Rayleigh or Rician distribution envelopes depending on the propagation environment where the receiver is used to account for the additional indirect received signal with either Rayleigh or Rician type channel, the received signal in equation 2 is redefined as

$$s(t)=a(t)e^{j(2\pi f_c t+\theta(t))}+\chi(t)+n(t) \quad (11)$$

where $a(t)e^{j(2\pi f_c t+\theta(t))}$ is the direct path signal, and $\chi(t)$ is the diffused complex signal at the receiver having real and imaginary parts with zero mean and a variance σ_x^2. The Rician factor, which is commonly used in experimental work and simulations, is defined as the ratio of direct received signal power to the diffused total power at the receiver and given by

$$K=\frac{a^2/2}{\sigma_x^2} \quad (12)$$

Since phase is still uniformly distributed for Rician and Rayleigh channels, (11) can be re-written as:

$$s(t) = R(t)e^{j(2\pi f_c t + \vartheta(t))} + n(t) \tag{13}$$

where ϑ is the phase to be estimated and distributed in $[-\pi, \pi)$ and $R = \sqrt{a^2(t) + |\chi(t)|^2}$ is the overall summation of direct and diffused envelope. This envelope results in either a Rayleigh or Rician distribution. Since Rayleigh distribution is a special case of Rician distribution, the received signal amplitude is distributed according to

$$p(R) = \frac{R}{\sigma_x^2} \exp\left[-\frac{R^2 + a^2}{2\sigma_x^2}\right] I_0\left(\frac{Ra}{\sigma_x^2}\right) \tag{14}$$

where, $I_0(.)$ is the zeroth-order modified Bessel function of the first kind. Using a new definition for the SNR to account for the extra energy in the received signal due to the indirect paths, SNR is redefined as:

$$\gamma_x = \frac{a^2/2 + \sigma_x^2}{\sigma_n^2} \tag{15}$$

For small K factors, where K=0 and a=0, (15) reduces to $\gamma_x = \frac{\sigma_x^2}{\sigma_n^2}$, which is the value for SNR of the Rayleigh channel. Similarly, for a very large K factor, (15) reduces to $\gamma_x = \frac{a^2/2}{\sigma_n^2}$ which is the SNR for a Gaussian channel derived in (6). Evaluating phase density and phase error estimation variance for Rician channels leads to a complete solution that include variance values for AWGN and Rayleigh channels. Using similar analysis as that used to obtain (8), the phase error density function for the Rayleigh channel [4] is given by:

$$P(\varphi)_N = \frac{1}{2\pi\left(1 + \gamma_x N \sin^2\varphi\right)} + \frac{\sqrt{\gamma_x N}\cos\varphi}{2\pi\left(1 + \gamma_x N \sin^2\varphi\right)^{3/2}} \left(\frac{\pi}{2} + \tan^{-1}\frac{\sqrt{\gamma_x N}\cos\varphi}{\left(1 + \gamma_x N \sin^2\varphi\right)^{1/2}}\right) \tag{16}$$

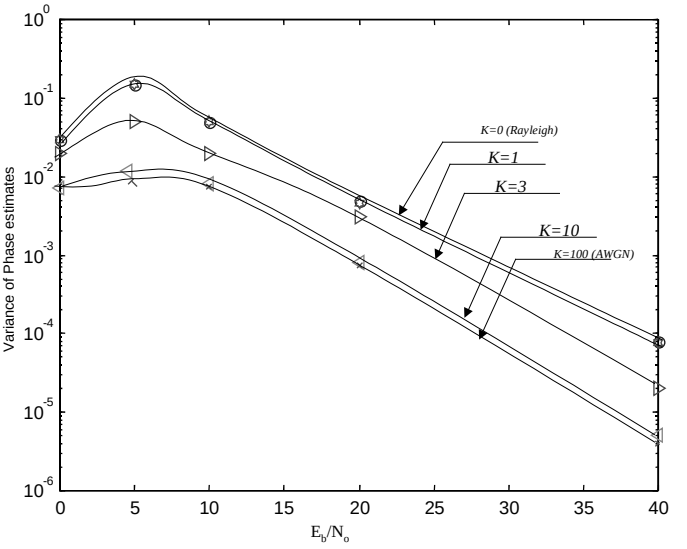

Figure 5. Variance of Phase in Rician Channel

The variance of the phase estimates for the Rician channel is given by:

$$\left\langle \varphi^2 \right\rangle = \frac{K+1}{\pi\gamma_x N} e^{-K} \int_{\theta=0}^{\pi} \int_{y=0}^{\infty} \varphi^2 y \exp\left[-\frac{y^2}{2}\left(1 + \frac{K+1}{\gamma_x N}\right)\right] .\left\{1 + y\sqrt{2\pi}\cos\varphi\left(e^{(y^2/2)\cos^2\varphi}\right)\left[1 - Q(y\cos\varphi)\right]\right\} .I_0\left(y\sqrt{\frac{2K(K+1)}{\gamma_x N}}\right) d\varphi dy \tag{17}$$

where $y = \frac{\sqrt{N}R}{\sigma_n}$. The variance in (17) cannot be solved in closed form, numerical methods must be used. Figure 5 shows a plot of this variance for several values of K for N=10 [2]. For large values of the Rician factor ($K = \infty$ most signals received are due to direct line-of-site transmission) the channel becomes an AWGN channel and the variance reduces to the CRB in equation 13. On the contrary, for small values of the Rician factor (K=0, most signals are due to diffused paths) the variance becomes an upper bound for phase estimates in the Rayleigh channel. This figure is very useful in predicting the performance of carrier phase tracking in Rayleigh, Rician, and AWGN. The figure can be used as a benchmark from which bounds can be obtained for the design of receiver links.

EFFECTS OF FREQUENCY RESIDUAL

In the prior analysis, it was assumed that phase carrier offsets are obtained after the signal has been corrected for carrier frequency offsets. In practical situations, there is a residual error that can be as high as 50-100 Hz resulting from inaccuracies of the frequency-offset algorithm used [5]. Such frequency-offset residual results in phase estimates that are not considered constant anymore during

the observation interval. As a result phase estimates using the algorithm shown in figure 1 will be biased by an amount of phase error that is a linear function of the index of symbols used during the observation interval, the phase bias due to the frequency offset is worst at the edge of the estimation and equal to $\theta(k) = 2\pi\Delta fTk$ degrees. Using (1), the argument of the output of the non-linearity in Figure 1 is given by:

$$\sum_{k=0}^{N-1} imag\{z_k^4\} = \sum_{k=0}^{N-1} e^{(4j(2\pi\Delta fTk+\theta+\phi_k))} \qquad (18)$$

where ϕ_k is a random variable describing the effect of data modulation, the averaging process in equation 1, makes ϕ_k phase contribution relatively small, since the data transmitted is random with all symbols having equal likelihood of being sent, so (18) can be simplified further to

$$\sum_{k=0}^{N-1} imag\{z_k^4\} = e^{(4j\theta)}(F(\Delta f, k, N) + \phi_k) \qquad (19)$$

where $F(\Delta f, k, N) = \frac{1}{4}\frac{\sin(2\pi 4N\Delta f/2)}{\sin(2\pi 4\Delta f/2)}$ is obtained using $\sum_{k=0}^{N-1} e^{(4j2\pi\Delta f)} \approx \frac{1}{4}\frac{\sin(2\pi 4N\Delta f/2)}{\sin(2\pi 4\Delta f/2)}$, equation 19 can be approximated by

$$\sum_{k=0}^{N-1} z_k^4 = e^{(4j\theta)}\frac{\sin(4\pi N\Delta f)}{\sin(4\pi\Delta f)} + \sigma_\theta \qquad (20)$$

where $E\{\sigma_\theta^2\} = NE\{\theta\}$. (20) Contains a useful signal and a noisy disturbance for the estimation process caused by the frequency offset Δf. Maximizing the useful part over *N* results in minimum effect caused by this frequency-offset Δf [6], resulting in an optimal observation interval length given by:

$$N_{ptimal} = \max\left\{\left(\frac{\sin(4\pi N\Delta f)}{\sin(4\pi\Delta f)}\right)^2\right\}_N \qquad (21)$$

So for a given frequency offset Δf Hz, there is an optimal value of the observation interval, which gives minimum variance for the phase estimates $\hat{\theta}$. For instance, using QPSK data rate of 10 ksps, and a Doppler or a residual frequency offset of 10, 20, 30, and 40 Hz, Figure 6 shows the optimal values that yield minimum variance of the phase estimates. For a frequency offset of 40 Hz ($\Delta fT = 4x10^{-3}$) the optimal observation interval for the phase algorithm in (1) is N_{ptimal}=100 symbols, while for an offset of 10 Hz, the optimal interval is N_{ptimal}=20 symbols.

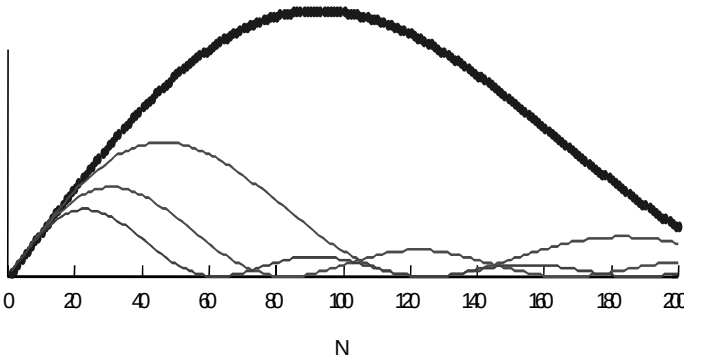

Figure 6. Optimal Observation Length

CONCLUSION

Phase error density functions were derived for an open loop carrier phase synchronizer operating in AWGN, Rayleigh, and Rician channels. Variances of estimates derived from such density function can be used by designers of receivers to determine worst conditions of BER deterioration due to phase estimator imprecise operation. Furthermore, the effect of frequency-offset residual on phase estimation accuracy was examined.

REFERENCES

1. W. Hagmann and J. Haberman, "On the Phase Error Distribution of an Open Loop Estimator", IEEE June 1988

2. Ruggero Reggiannini, "A Fundamental Lower Bound to the Performance of Phase Estimator Over Rician Fading Channels", IEEE Transaction on Communications, Vol. 45 No. 7, July 1997

3. M. Nezami and R. Sudhakar, "New Schemes for 16-QAM Symbol Recovery", Eurocom2000 Münich, Germany 17-19 May 2000

4. M. Nezami and R. Sudhakar, "M-QAM Digital Symbol Timing Synchronization in Flat Rayleigh Fading Channels", PRMIC, Osaka Japan, Nov 1999

5. M. Nezami and R. Sudhakar, "DSP Algorithms for Carrier Offset Estimation and Correction", ICSPAT, Orlando, Florida, USA, November 1999

6. Greet De Jonghe and Marc Moeneclaey, " Optimal averaging filter length of the Viterbi @ Viterbi carrier synchronizer for a given frequency offset", IEEE, 1994.